Letters

IOP Publishing

Journal of Physics: Condensed Matter

J. Phys.: Condens. Matter **32** (2020) 20LT01 (6pp)

https://doi.org/10.1088/1361-648X/ab6f85

Letter

Electron correlations and memory effects in ultrafast electron and hole dynamics in VO_2

Jose Mario Galicia-Hernandez[1,2], Volodymyr Turkowski[1], Gregorio Hernandez-Cocoletzi[2] and Talat S Rahman[1]

[1] Department of Physics, University of Central Florida, Orlando, FL 32816, United States of America
[2] Instituto de Fisica Ing. Luis Rivera Terrazas, Benemerita Universidad Autonoma de Puebla, Puebla 72550, Mexico

E-mail: talat.rahman@ucf.edu

Received 19 October 2019, revised 20 December 2019
Accepted for publication 24 January 2020
Published 20 February 2020

Abstract

By applying an approach based on time-dependent density functional theory and dynamical mean-field theory (TDDFT+DMFT) we examine the role of electron correlations in the ultrafast breakdown of the insulating M_1 phase in bulk VO_2. We consider the case of a spatially homogeneous ultrafast (femtosecond) laser pulse perturbation and present the dynamics of the melting of the insulating state, in particular the time-dependence of the excited charge density. The time-dependence of the chemical potential of the excited electron and hole subsystems shows that even for such short times the dynamics of the system is significantly affected by memory effects—the time-resolved electron–electron interactions. The results pave the way for obtaining a microscopic understanding of the ultrafast dynamics of strongly-correlated materials.

Keywords: vanadium dioxide, dynamical mean-field theory, ultra-fast dynamics

Supplementary material for this article is available online

(Some figures may appear in colour only in the online journal)

1. Introduction

It is well known that the static (equilibrium) properties of strongly correlated materials can be easily tuned by changing the temperature, pressure and geometry of the system. More recently, Cavalleri *et al* [1] have shown that an ultrafast laser pulse can also cause an insulator-to-metal transition (IMT), as recorded by a large change of conductivity, in VO_2 at the 100 fs time scale. Time-resolved photoemission electron spectroscopy [2, 3], ultrafast electron diffraction and infrared transmissivity [4] and ultrafast temperature- and fluence-dependent optical spectroscopy and x-ray scattering [5] measurements confirmed that the insulating gap during the IMT closes without changing the lattice structure of VO_2 during the first few hundred femtoseconds after the excitation. Besides very rich and interesting physics, such tunability with an ultrafast pulse has great potential application in ultrafast technologies, such as switches [6–8], microelectromechanical systems (MEMS) [9], smart windows [10] and biosensors [11]. Therefore, understanding of the ultrafast properties of VO_2 and other strongly correlated materials is essential from both fundamental and technological perspectives.

After many years of theoretical and experimental investigations the static (equilibrium) properties of bulk VO_2 are now well-understood. It is known experimentally that this system undergoes IMT with structural change from the monoclinic M_1 to the rutile (R) phase with $T_c \approx 340$ K [12] (the electronic bandgap in the insulating phase ~0.6 eV [13]). Theoretical debate on the subject has culminated with the efforts of Brito *et al* [14] who demonstrated using a combination of density functional theory (DFT) and dynamical mean field theory (DMFT) that strong electron–electron correlations play a

dominant role in the IMT in VO_2. This transition might be characterized as a Mott transition in the presence of a strong inter-site exchange that leads to splitting of the a_{g1} states within the vanadium dimers. Importantly, contrary to LDA + U [15–17], another popular approach applied to strongly correlated systems, DFT+DMFT reproduce a nonmagnetic ground state in the M_1 phase (LDA + U gives an antiferromagnetic one [18]) and describes the temperature-induced metallization accompanied by the M_1–R structure change at fixed value of the local Coulomb electron–electron repulsion U (LDA + U gives an insulating phase for both M_1 and rutile structures). These successes of DFT+DMFT can be traced to the inclusion of dynamical (time-resolved) on-site electron–electron interactions (see, e.g. [14, 17–21]). The role of electron correlation should be even more explicit when the system is subjected to an ultrafast laser pulse taking it far from equilibrium and triggering excited state charge dynamics, whose analysis would greatly benefit from incorporation of DMFT, as we shall see.

As a matter of fact, nonequilibrium (ultrafast) properties of VO_2 remain the subject of theoretical investigations and the search for appropriate techniques continues as new experimental data need to be understood. In fact, the body of experimental data on the femtosecond metallization in VO_2 (transition from the insulating M_1 phase to the metallic, so called $\mathcal{M}$, phase with the same lattice structure) keeps growing (for over-review and references, see [22]), thanks to tremendous advances in the field. Briefly, the kinetics of the $M_1 \rightarrow \mathcal{M}$ phase transition corresponds to an electron temperature driven transition with activation energy of 304 ± 109 meV. The response of the system depends on the perturbation fluence and can be basically one of the three types: (1) f_ at laser pump fluences below ~3 mJ cm^{-2}, VO_2 behaves like a Mott insulator with a small increase in conductivity succeeded by recovering of the insulating state; (2) at fluences between 3 and 8 mJ cm^{-2} the excited system achieves the $\mathcal{M}$ phase (15%–20% of the total volume at fluence 8 mJ cm^{-2}). The state is characterized by collapse of the bandgap and a dramatic increase in conductivity. It was shown by Wegkamp *et al* [2] that the IMT emission has contributions from states below and above the Fermi energy, indicating the existence of both metallic and insulating domains during the transition (with estimated electron and hole lifetimes $\tau_e \sim 160$ fs, $\tau_h \sim 210$ fs); (3) at fluences above 8 mJ cm^{-2} the excitation creates both $\mathcal{M}$ and emerging R domains, while at fluences 20 mJ cm^{-2} the R domains become dominant.

Another significant aspect of these ultrafast pump-probe experiments is their ability to resolve response of the system at tens of fs timescale [23], providing the opportunity to trace the origin of features observed at the 100 fs and ps response. Note that already from the few-femtosecond extreme UV transient absorption spectroscopy (FXTAS) measurements, it has been proposed that the IMT in VO_2 might take place at timescales shorter than 100 fs, more in the $20 - 32$ fs [4] range. Furthermore, the FXTAS data suggest involvement of the often-neglected oxygen p-states in the ultrafast dynamics of VO_2 [24], raising questions about the role of strong electron–electron correlations in determining the time-resolved vanadium and oxygen orbital-occupancies during the IMT.

Accurate theoretical analysis of excited state charge dynamics are, however, challenging. Unsurprisingly, until recently the dynamics of the IMT in VO_2 was analyzed mostly in terms of phenomenological models that either neglect correlation effects or take them into account in an adhoc way [25–28]. To our knowledge, the first systematic *ab initio* (DFT + U) study, supplemented with the Boltzmann equation, which allows meaningfully incorporation of correlation effects in the ultrafast charge dynamics of VO_2 was performed by He and Millis [29], who showed that the system may indeed undergo an intermediate fs transition into a metastable $\mathcal{M}$ phase, with characteristics time scales for the electron and hole dynamics. To explain the nature of this phase transition, they proposed the following scenario. Initially the excited electrons and holes relax rapidly (~1–5 fs) to a pseudothermal distribution with one common temperature and different chemical potentials, as defined by the pulse energy and the number of initially created electrons and holes. Next, the pseudothermal distribution evolves in ~100 fs into a thermal distribution at a common temperature and chemical potential. At even longer (ps) times the system can be in two states, i.e. the Hartree–Fock energy might have two minima, one corresponding to the equilibrium state and the other to the metastable metallic state with special occupancy of d-orbitals. Furthermore, at the $M_1 \rightarrow \mathcal{M}$ transition all low-energy vanadium t_{2g} bands (the initially partially occupied (split by the gap) $d_{x^2-y^2}$ and empty d_{xz}, d_{yz} bands) become partially occupied. Similarly, the gaps in the split oxygen p-bands also close during the $M_1 \rightarrow \mathcal{M}$ transition.

The interesting results obtained by He and Millis lead to the questions: would inclusion of time-resolved electron–electron interaction, as inherent in DMFT, allow further insights into the role of electron correlations in the IMT in VO_2? Is it possible to track the excited state charge dynamics on an *ab initio* basis rather than relying on the Boltzmann equation? To address these issues, one could apply nonequilibrium DMFT [30, 31], except that it is computationally prohibitive, particularly for a system that may be spatially nonhomogeneous and contains more than few (1–2) d-orbitals. A more computationally feasible alternative is our recently developed TDDFT+DMFT that combines *ab initio* and many-body theory approaches [32]. It takes into account time-resolved electron–electron interaction (memory effects) via the XC potential (kernel) that is derived from the DMFT charge susceptibility for an effective Hubbard model. Being an effective theory of one function—charge density—it is computationally efficient. Another advantage of the approach is its suitability for examining spatially-resolved charge dynamics in strongly correlated material such as VO_2, which display striking characteristics but have not yet received much attention.

In this work, we apply TDDFT+DMFT to examine the following for VO_2: (1) initial (~10 fs) stage orbital-resolved charge dynamics; (2) effect of the memory on the time-dependence

of the excited electron and hole chemical potentials. In the next section we provide some details of our computational approach. This is followed in section 3 by results and discussion and section 4 summarizes our conclusions.

2. TDDFT+DMFT approach and the computational details

In TDDFT+DMFT, one begins with DFT calculations of the ground state properties: the relaxed lattice structure, the electronic spectrum, the density of states (DOS) and the static Kohn–Sham wave functions. In the next step, through application of DFT+DMFT [33] a corrected excitation spectrum, DOS and electron charge susceptibility are obtained, which include the effects of electron correlations. The last quantity is then used to construct the TDDFT XC kernel (for details, see supplementary information (stacks.iop.org/JPhysCM/32/20LT01/mmedia), section I). Finally, the DFT+DMFT spectrum and the XC kernel enter the TDDFT Kohn–Sham equation. The solution of this equation in the presence of an external perturbation gives the time- and space-dependent excited electron charge density, state occupancies and other quantities of interest. Below, we give more details of the calculations during these three stages.

The DFT calculations with the Perdew–Wang LDA XC potential and norm-conserving semi-local pseudopotentials were performed with the Quantum ESPRESSO package [34] ($9 \times 9 \times 9$ Monkhorst–Pack k-points mesh in the first Brillouin zone, cut-off energy 70 Ry). The dimerization of the vanadium atoms was obtained by doubling the unit cell in the C_R direction (in figure 1(a) we show a vanadium-atom dimer encircled by green curve, and two vanadium atoms that belong to the nearest dimers are encircled by an orange curve).

The DFT+DMFT calculations were performed by solving an effective five d-band (V) and three p-band (O) Hubbard problem with the on-site Coulomb repulsion and exchange energies $U = 4\,\mathrm{eV}$ and $J = 0.65\,\mathrm{eV}$ on the vanadium atoms and the inter-site (same-orbital same-spin) interaction within the vanadium dimers $V = 1\,\mathrm{eV}$. The impurity problem was solved with multi-orbital iterative perturbation theory (MO-IPT) approach (see, e.g. [33]).

To study the response of the system, we solved the TDDFT Kohn–Sham equation with the DMFT spatially-local non-adiabatic XC kernel defined in supplementary information, section II. The solution of the Kohn–Sham equation was obtained by expanding the time-dependent wave function, which is expanded in terms of the static d-orbital Kohn–Sham wave functions (for details, see supplementary information, section II).

3. Results and discussion

3.1. Ground-state properties

The results for the total and projected vanadium-atom d-orbital as well as the next by strength oxygen p-orbital DFT DOS are shown in figures 1(b) and (c) which establish that the optically active orbitals near the Fermi energy have predominantly

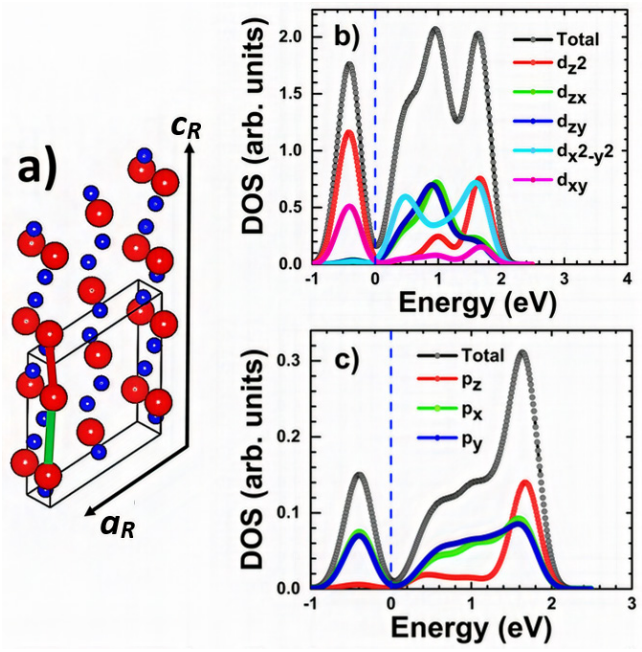

Figure 1. (a) The M_1 unit cell with the vanadium and oxygen atoms shown in red and blue, correspondingly. A pair of V-dimer atoms along the c_R axis is marked by a green bond, while two unpaired atoms—by the red. (b) V-atom total and projected d-orbital DOS obtained with the DFT calculations. Dashed line corresponds to the Fermi energy. (c) The same as in previous figure for the p-orbital DOS of one the two non-equivalent O atoms.

d-wave symmetry. Another important DFT result is the chain dimerization of the V-atoms in the M_1 phase (figure 1(a)). As expected our DFT results find the low temperature phase to be metallic, in disagreement with experimental observations, as we have discussed in the Introduction. Note that our DFT results are in agreement with those that have already been presented in the literature [13, 17] and are included here for completeness.

A first success of the DFT+DMFT approach is that it reproduces the experimentally-observed gap (our result for the gap 0.67 eV is in a rather good agreement with the experimental value ~0.6 eV (see, e.g. [13, 35])). It should be noted that after performing a single-site DMFT calculation, we include inter-site interactions [14] by taking into account the intra-dimer, same-orbital interaction (described by the last term in the Hamiltonian equation (1)) as a perturbation (since $\mathrm{V} \ll \mathrm{U}, \mathrm{U}-\mathrm{J}, \mathrm{U}-2\mathrm{J}$). The bands thereby acquire the necessary bonding and anti-bonding splitting, leading to opening of the gap in the DOS. It is important to stress that the DMFT spectrum has no gap if the intra-dimer repulsion V is zero (see also [14]). The total DFT and DFT+DMFT DOS are shown in figure 2. Some difference in the shape of the DMFT DOS from other works (see, e.g. [14, 20, 21]) can be related to the difference in the used impurity solver.

3.2. Ultrafast (100 fs) 'spatially-average' response

In a naïve band-insulator picture (figure 3(a)), the ultrafast response of the electronic system would take place in four stages. The excited electrons (stage I) would fill out the

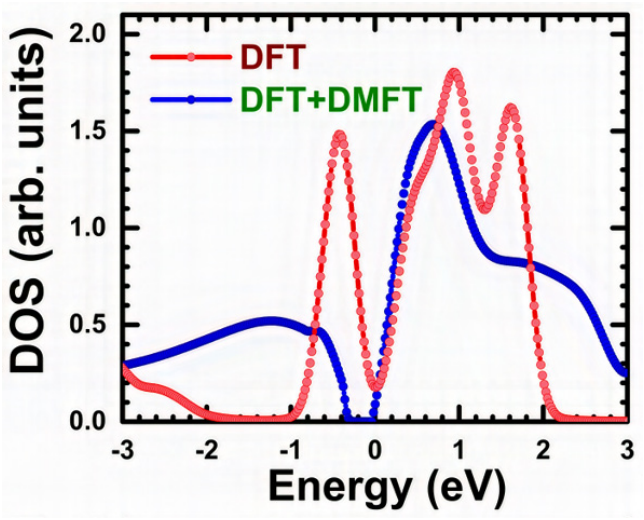

Figure 2. The total DFT and DFT+DMFT ($U = 4$ eV, $J = 0.65$ eV) DOS for the d-orbital subsystem of VO_2. The Fermi energy is set to 0 eV.

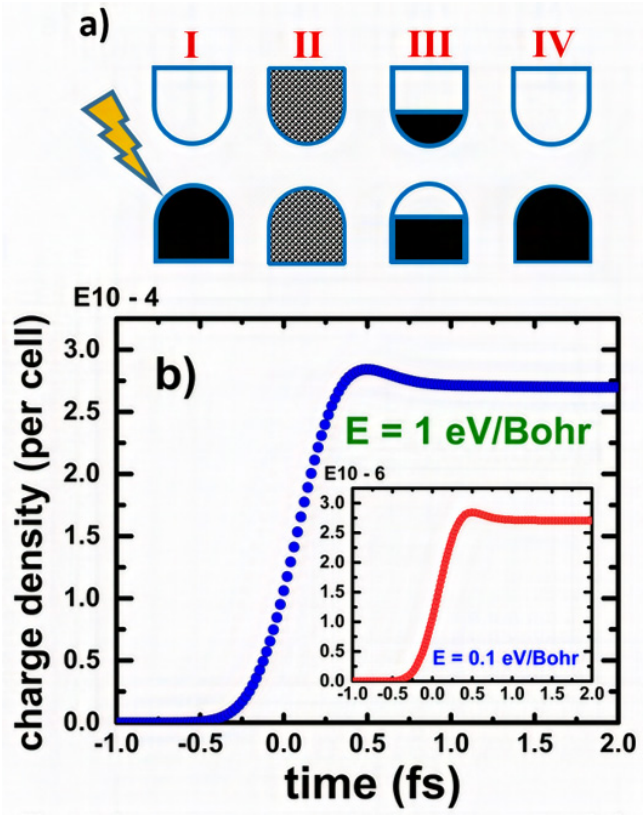

Figure 3. (a) Four-stage ultrafast dynamics: (I) laser-pulse field is applied to the unperturbed system; (II) nonequilibrium metallization; (III) quasi-equilibrium metallic state; (IV) the charges relax back to the equilibrium state. (b) The excited charge density as function of time in the case of 0.82 fs excitation and field magnitudes $E = 1$ eV/Bohr and $E = 0.1$eV/Bohr, or fluences 0.1 mJ cm^{-2} and 0.001 mJ cm^{-2} (inset).

continuum of the conduction band states (stage II), then settle down at the bottom of the conduction band (stage III), forming quasi-static metallic state with the Fermi level defined by the number of excited charges before relaxing to their ground

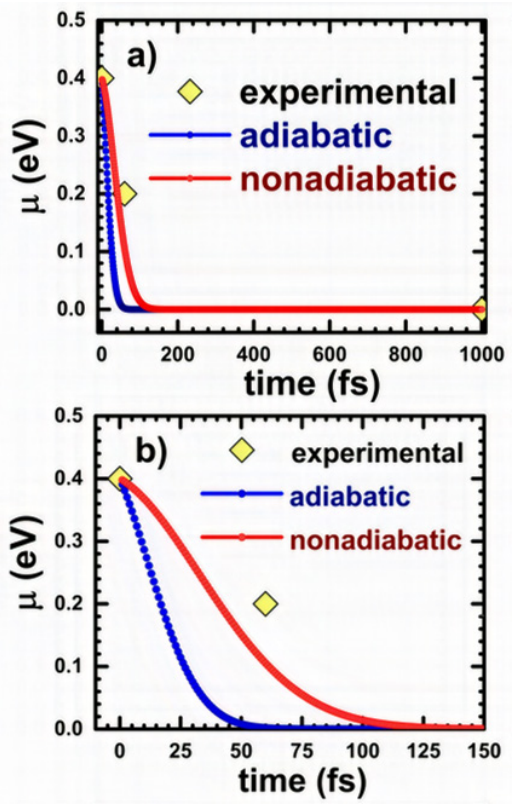

Figure 4. (a) Evolution of the chemical potentials in the cases of adiabatic and non-adiabatic solutions and the excitation parameters in figure 3. Squares are the experimental data [4]. (b) The same at times below 200 fs.

(valence-band), and consequently recombine with holes (stage IV). Though, the femtosecond response of strongly correlated systems is significantly affected by the local Coulomb interaction as compared to the band insulators, indications of an intermediate metallic state (stage III) with insulating M_1 lattice structure of VO_2 have been demonstrated (see, for example, [2, 4]). In particular, the relaxation to the quasi-static metallic phase takes place at the timescale of order 100 fs [4]. To test this possibility and to analyze other features of the ultrafast response of VO_2, we applied the TDDFT+DMFT with a spatially-homogeneous laser pulse perturbation.

The excited charge density was obtained by propagating the Liouville equation for the density matrix-elements in time (density-matrix version of TDDFT) and calculating total occupancy of the conduction states as function of time (defined as sum of the diagonal matrix elements for the conduction bands, see supplementary information, section II). As shown in figure 3(b) the charge-pumping stage takes place at the 1 fs timescale. Results of further analysis for different pulse duration (not shown) demonstrate that the pumping stage happens during the time of the pulse duration. The number of excited charges is proportional to the magnitude of the field (see inset in the figure 3(b) for the case of a weaker field). Since the results for two different field magnitudes demonstrate similar dynamics, we choose $E = 1$ eV/Bohr for the rest of the anaysis presented here. It is important to mention that the pulse fluences used in the calculations (0.1 mJ cm^{-2} and 0.001 mJ cm^{-2})

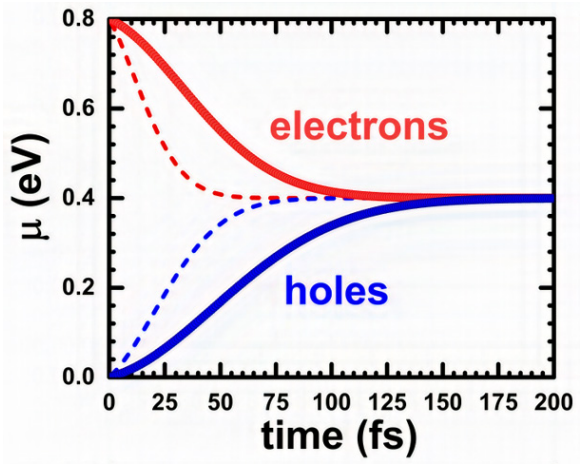

Figure 5. Time-dependencies of the electron and hole chemical potentials in the cases of adiabatic (dashed curves) and nonadiabatic (solid curves) approximations.

are rather weak and are not sufficient to generate lattice transformation, i.e. we analyze the case of the excited system with the M_1 band structure.

We have also calculated the time-dependence of the excited electron and hole chemical potentials, by tracking the evolution of the corresponding Fermi energies. It was done by using the same approach as in the calculation of the excited charge (figure 3(b))—we solved the Liouville equation for the density matrix elements and calculated the excited charge density by performing summation of the diagonal matrix elements for the excited states, calculating total charge density and identifying the energy (defined by the band momenta) below which 90% of excited (electron and hole) charges are accommodated. In figure 4 we show the results for the time evolution of the chemical potential for the electrons excited into the 'conduction' band for two types of the XC kernel potential: the nonadiabatic and its adiabatic approximation, i.e. $f_{\rm XC}(r,r',\omega) = f_{\rm XC}(r,r',\omega=0)$.

Figure 4 attests that relaxation to the metallic state takes place at times ~50 fs, in agreement with experimental data [4]. Time-dependencies of the chemical potential figure 4 show that the non-adiabatic effects slow-down the relaxation processes (see also [29] in which the adiabatic solution in the framework of the Boltzmann equation was considered). In the TDDFT+DMFT case, the nonadiabatic solution is closer to the experimentally estimated relaxation times, pointing to the importance of memory effects. Though the nonadiabatic solution for the chemical potential is in better agreement with the experimental values as compared to those obtained in the adiabatic limit, some discrepancy between the experiment and theory still exists (see the square at time ~60 fs). We expect a further improvement of the theoretical results after inclusion of spatially non-local interactions into the TDDFT+DMFT XC kernel (Equation (SI.14) in the Supplementary Information). Similar results were obtained for the hole relaxation (figure 5), where again the non-adiabaticity slows down the relaxation. It should also be noted that the above obtained time of the IMT ~50 fs is not far from the lowest estimate so-far obtained from experiments (20–32 fs) [23].

4. Conclusions

In this manuscript, we have applied the nonadiabatic TDDFT+DMFT approach to study the ultrafast electronic response in the M_1 insulating phase of VO_2. It was shown that the electronic correlations, including the memory effects play an important role already at the fs timescale. We have calculated the excited charge density as function of time in the case of a homogeneous laser pulse excitation. As it follows from our calculations, the charge pumping takes place almost immediately after the excitation, and the system relaxes to the quasi-static metallic state at times ~50 fs in agreement with experimental data. Inclusion of the memory effects slows down the chemical potential equilibration as compared to the adiabatic solution.

We plan to extend the analysis on the case of longer times, including the phonon and other temperature effects (like transformations of the lattice structure). This hopefully will help to build a complete 0-to-ps scenario of the charge dynamics in VO_2 during the IMT as function of time, a very important goal from both fundamental and technological points of view.

Acknowledgments

We thank R D Averitt, W H Brito and J Staehler for very helpful communications. We acknowledge the US DOE for a partial support under Grant DE-FG02-07ER46354. JMGH would like to thank CONACYT (Mexico) for support through the Postdoctoral Fellowship Program (Scholarship # 23210).

ORCID iDs

Jose Mario Galicia-Hernandez https://orcid.org/0000-0002-0323-3761
Volodymyr Turkowski https://orcid.org/0000-0003-0762-0002

References

[1] Cavalleri A, Tóth C, Siders C W, Squier J A, Ráksi F, Forget P and Kieffer J C 2001 *Phys. Rev. Lett.* **87** 237401
[2] Wegkamp D *et al* 2014 *Phys. Rev. Lett.* **113** 216401
[3] Laverock J, Kittiwatanakul S, Zakharov A A, Niu Y R, Chen B, Wolf S A, Lu J W and Smith K E 2014 *Phys. Rev. Lett.* **113** 216402
[4] Morrison V R, Chatelain R P, Tiwari K L, Hendaoui A, Bruhács A, Chaker M and Siwick B J 2014 *Science* **346** 445
[5] Gray A X *et al* 2018 *Phys. Rev.* B **98** 045104
[6] Servin R, Jin-Hyung P, In-yeal L, Jeong Min B, Kyung Soo Y and Gil-Ho K 2014 *J. Phys. D: Appl. Phys.* **47** 295101
[7] Markov P, Marvel R E, Conley H J, Miller K J, Haglund R F and Weiss S M 2015 *ACS Photonics* **2** 1175
[8] Pergament A, Crunteanu A, Beaumont A, Stefanovich G and Velichko A 2016 (arXiv:1601.06246)
[9] Merced E, Torres D, Tan X and Sepúlveda N 2015 *J. Microelectron. Syst.* **24** 100
[10] Liu C, Balin I, Magdassi S, Abdulhalim I and Long Y 2015 *Opt. Express* **23** A124

[11] Nie G, Zhang L, Lei J, Yang L, Zhang Z, Lu X and Wang C 2014 *J. Mater. Chem.* A **2** 2910
[12] Marezio M, McWhan D B, Remeika J P and Dernier P D 1972 *Phys. Rev.* B **5** 2541
[13] Eyert V 2002 *Ann. Phys., Lpz* **11** 650
[14] Brito W H, Aguiar M C O, Haule K and Kotliar G 2016 *Phys. Rev. Lett.* **117** 056402
[15] Chen S, Liu J, Luo H and Gao Y 2015 *J. Phys. Chem. Lett.* **6** 3650
[16] Budai J D *et al* 2014 *Nature* **515** 535
[17] Liebsch A, Ishida H and Bihlmayer G 2005 *Phys. Rev.* B **71** 085109
[18] Eguchi R *et al* 2008 *Phys. Rev.* B **78** 075115
[19] Weber C, O'Regan D D, Hine N D M, Payne M C, Kotliar G and Littlewood P B 2012 *Phys. Rev. Lett.* **108** 256402
[20] Biermann S, Poteryaev A, Lichtenstein A I and Georges A 2005 *Phys. Rev. Lett.* **94** 026404
[21] Belozerov A S, Korotin M A, Anisimov V I and Poteryaev A I 2012 *Phys. Rev.* B **85** 045109
[22] Otto M R *et al* 2019 *Proc. Natl Acad. Sci.* **116** 450–5
[23] Jager M F *et al* 2017 *Proc. Natl Acad. Sci.* **114** 9558
[24] Dietze S H, Marsh M J, Wang S, Ramírez J G, Cai Z H, Mohanty J R, Schuller I K and Shpyrko O G 2014 *Phys. Rev.* B **90** 165109
[25] Hilton D J, Prasankumar R P, Fourmaux S, Cavalleri A, Brassard D, El Khakani M A, Kieffer J C, Taylor A J and Averitt R D 2007 *Phys. Rev. Lett.* **99** 226401
[26] Madan H, Jerry M, Pogrebnyakov A, Mayer T and Datta S 2015 *ACS Nano* **9** 2009
[27] Shekhawat A, Papanikolaou S, Zapperi S and Sethna J P 2011 *Phys. Rev. Lett.* **107** 276401
[28] Vikhnin V S, Lysenko S, Rua A, Fernandez F and Liu H 2007 *Opt. Mater.* **29** 1385
[29] He Z and Millis A J 2016 *Phys. Rev.* B **93** 115126
[30] Freericks J K, Turkowski V M and Zlatic V 2006 *Phys. Rev. Lett.* **97** 266408
[31] Aoki H, Tsuji N, Eckstein M, Kollar M, Oka T and Werner P 2014 *Rev. Mod. Phys.* **86** 779
[32] Turkowski V and Rahman T S 2017 *J. Phys.: Condens. Matter* **29** 455601
[33] Kotliar G, Savrasov S Y, Haule K, Oudovenko V S, Parcollet O and Marianetti C A 2006 *Rev. Mod. Phys.* **78** 865
[34] Giannozzi P *et al* 2009 *J. Phys.: Condens. Matter* **21** 395502
[35] Verleur H W, Barker A S Jr and Berglund C N 1968 *Phys. Rev.* **172** 788